

FreqX: What neural networks learn is what network designers say.

Zechen Liu¹
Wuhan University
zecliu@whu.edu.cn

November 28, 2024

Abstract

Personalized Federal learning(PFL) allows clients to cooperatively train a personalized model without disclosing their private dataset. However, PFL suffers from Non-IID, heterogeneous devices, lack of fairness, and unclear contribution which urgently need the interpretability of deep learning model to overcome these challenges. These challenges proposed new demands for interpretability. Low cost, privacy, and detailed information. There is no current interpretability method satisfying them. In this paper, we propose a novel interpretability method *FreqX* by introducing Signal Processing and Information Theory. Our experiments show that the explanation results of *FreqX* contain both attribution information and concept information. *FreqX* runs at least 10 times faster than the baselines which contain concept information.

Introduction

Personalized Federated Learning(PFL) enables different data owners to cooperatively train a personalized model without sharing their dataset. The regular paradigm is that clients train a local model using their own data and local devices, and then send their trained models to a center server. The server aggregates their models and sends the aggregated model back. Clients and the server repeat these operations until the model converges McMahan et al. [2017]. However, this causes PFL to suffer from numeric problems such as Non-IID Li et al. [2020], personalization Li et al. [2021a], device heterogeneous Xu et al. [2023], Li et al. [2023], lack of fairness Rafi et al. [2024]. These problems urge the researchers to efficiently provide a good explanation for DNNs in PFL.

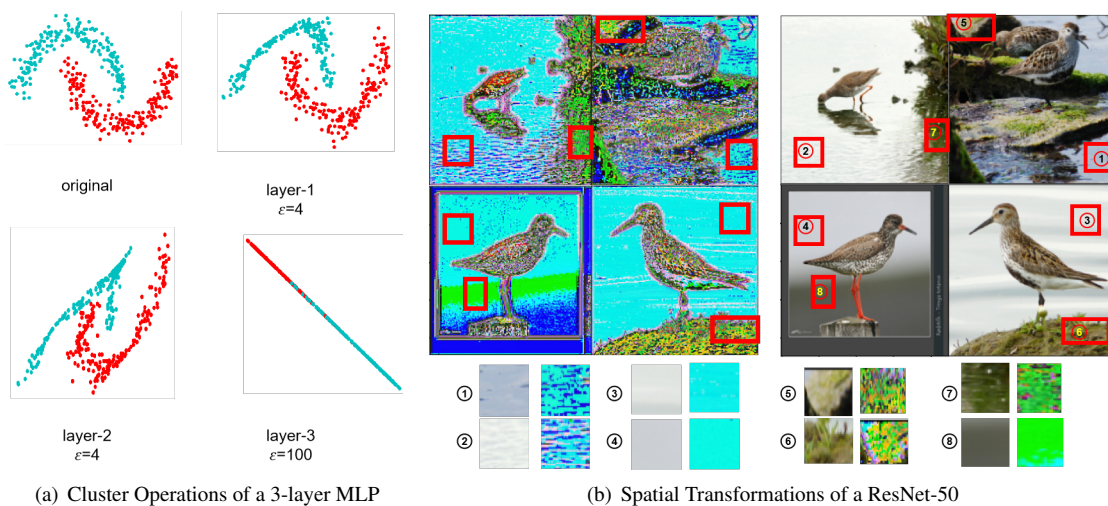


Figure 1: 1(a): The cluster operations of a 3-layer MLP towards a simulated binary classification dataset with only two features(ϵ denotes the augmentation coefficient). 1(b): We visualize the spatial transformation operations of Resnet-50.

Without an efficient interpretability method, researchers now are adopting re-training Zhang et al. [2023] or alignment-based Zhu et al. [2021], Chen et al. [2023], Li et al. [2021a] methods to extract the desired information from the aggregated model. Lack of interpretability blocks them from designing more explainable and economical algorithms. For fairness FL, especially collaboration fairness, researchers categorize the clients into groups Chaudhury et al. [2022], Rafi et al. [2024] and do retraining to estimate the contribution of each client or use individualized assessment. These methods are costly (such as the Shapley-Value based method with a complexity of $O(n!)$) or unreality (The basic assumptions are hard to achieve in reality) Rafi et al. [2024].

So if we can reveal the content that deep networks have learned in PFL, we can then vigorously advance the resolution of the aforementioned issues. However, PFL raises new limitations for explanation methods: 1) Due to the heterogeneity of the local devices, **the cost of the explanation method should be as low as possible** to avoid sampling bias or long time waiting Xu et al. [2023]. Additionally, **the cost will accumulate** if an explanation method needs to be performed at each round of aggregation. 2) The explanation results should **contain detailed information of what the network learned**. Because we need to calculate the contributions of participants. 3) The explanation method **should not rely on the knowledge of the entire dataset**. Because the training data is separated into different clients and the data can not be shared, each client has little prior knowledge. Although the interpretability of neural networks has been deeply studied, there are still deficiencies in PFL. Neither feature attribution-based methods Srinivas and Fleuret [2019] nor concept-based methods Fel et al. [2023], Sun et al. [2023], which are the mainstream explanation methods. Feature attribution is poor of detailed information of what the network learned (*limitation2*) and the other relies on prior knowledge of the entire dataset (*limitation3*).

Motivated by these issues, and inspired by signal processing Wright et al. [2022], Jianxun Zhao [2018], information bottleneck theory Alemi et al. [2017], Kawaguchi et al. [2023], prototype learning Qin et al. [2023a,b] and previous works Ley et al. [2023], Smith [1997], Konforti et al. [2023], we propose a new method called FreqX which satisfies the limitations by explaining how a network classifies the samples layer by layer.

There is another significant issue in the interpretability field, the metrics. The two major metrics, Del-Ins Game and Remove And Retrain (ROAR) are both criticized for their different weakness. The ROAR is criticized because it needs to retrain the model, some researchers argue Yang et al. [2023a] that it is not faithful. Del-Ins Game will introduce new edge signals into the picture which will frustrate the model Srinivas and Fleuret [2019]. That's true. See Fig.2 as an example, We start with a green square, and then we remove the pixels from the corners of the square we can get a triangle. What's more, by removing pixels we can also get a little person who is playing basketball! Therefore, the deletion operation in the time domain is not real *deletion*. It may introduce new information that frustrates the network. We can see in the frequency domain, that the deletion operation introduces new signals with different frequencies into the picture. So, inspired by Fourier transformation, we turn the deletion operation into the frequency domain.

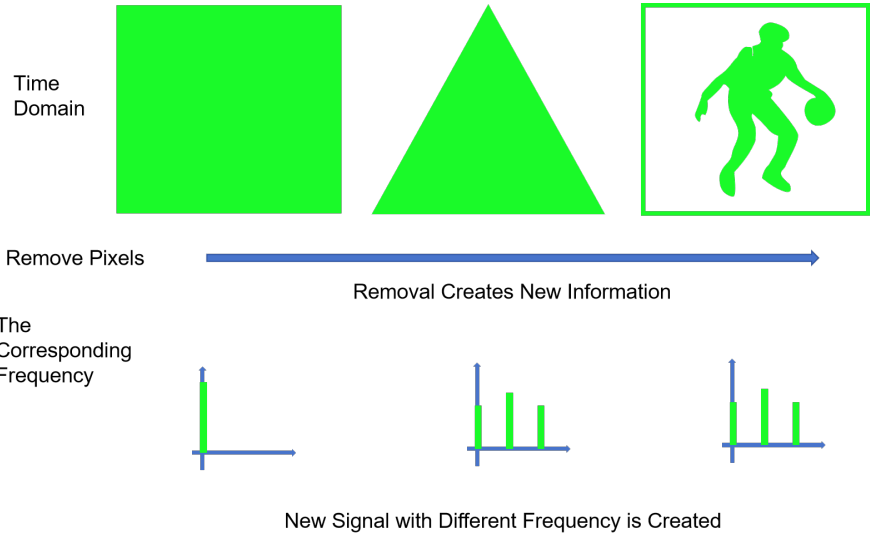


Figure 2: The deletion operation in the time/space domain is not real **Deletion**. It introduced new signals.

According to signal processing, Fourier Transformation de-composites the signal into different signals with different frequencies, and the deletion of those signals will not introduce new signals. Therefore, we propose

a new measure called FreqDIG(Frequency Deletion and Insertion Game) whose deletion is a real deletion that will not introduce extra signals like time domain. We transform the interpretability methods in the time domain into the frequency domain with the equation below:

$$S_f(u, v) = \sum_y \left(\sum_x S_t(x, y) e^{-j \frac{2\pi}{N} x u} \right) e^{-j \frac{2\pi}{N} y v} \quad (1)$$

Where S_f means the score of frequency, S_t means the score in the time domain. After transforming the scores into the frequency domain, We observed that the feature frequencies and noise frequencies differed greatly in their effects on the models. As shown in Fig.3 and Fig.6 In the time domain, we need to set more than 30% pixels(which are regarded as important pixels by the interpretability algorithms) to zero to decrease the model performance. However, in the frequency domain, deleting 10% important frequencies will completely change the network’s prediction. (The network here is ResNet-50). In contrast, deleting the noise frequency will slightly change the network output, and even increase the confidence of the original judgment. In the third figure, even if only 10 frequencies are deleted, the network’s reaction is changed significantly. Therefore, we draw the conclusion that the network is sensitive to frequency. More arbitrarily, the CNN network learned frequency information.

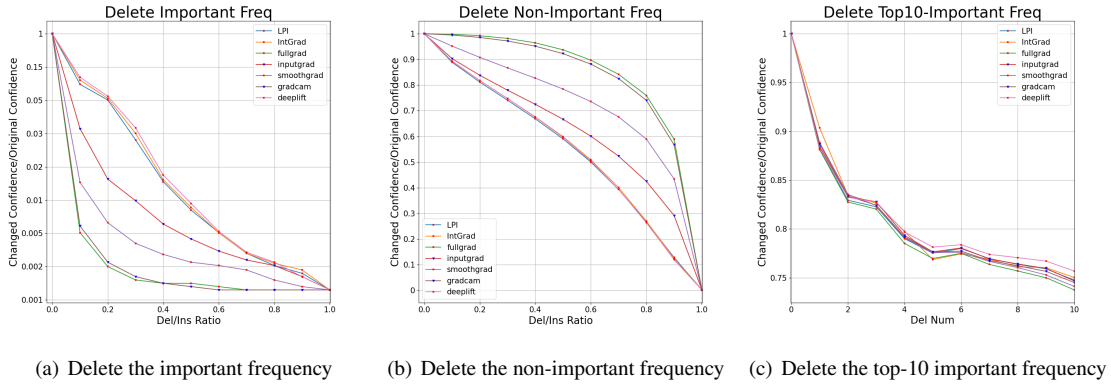


Figure 3: The FreqDIG.

Therefore, we turn the key point of interpretability from the time domain into the frequency domain.

It is demonstrated that classification networks cluster the samples in hyper-spaceKonforti et al. [2023], and information bottleneck theory demonstrated that the networks can filter the noise and extract the important information. To the best of our knowledge, we are the first team to reveal the filter and extract operations in the original sample space which is more friendly for humans to understand.

As shown in Fig.1(a), the network gradually separates two classes by allocating two contrast vectors. As shown in Fig.1(b), after the transformation operations are mapped into the original space, we can see ResNet-50 maps similar concepts to nearby spaces such as “river”(labeled as 1,2), “sky”(labeled as 3,4), “ground”(labeled as 5,6), and “grass”(labeled as 7,8). Based on the transformation, we can turn our explanation result into the feature-attribution-based method. Additionally, the transformation contains concept information. FreqX extracts both **two types** of information within only **10 minutes**.

Our contributions can be summarized as follows:

- We propose a novel explanation method that satisfies the limitations of PFL. To the best of our knowledge, we are the first team that can map the extract/filter operations of a network to the original sample space.
- We demonstrate that the proposed method can be converted to existing feature attribution methods and our explanation result contains concept information
- We demonstrate that our method can be aggregated into global explanations and applied in PFL.

| Notations | Meanings |
|---------------|-------------------------------------|
| x_{ci} | i -th sample with label c |
| v | a vector |
| w | weights of a neuron |
| x' | sample after spatial transformation |
| M_i | The i -th row of matrix M |
| σ | activation function |
| ε | augmentation coefficient |

Table 1: Important Notations in Method

Related Works

Personalized Federated Learning

Personalized federated learning is challenging because the participants often have different situations including different distribution Gao et al. [2022] and computational resources Xu et al. [2023]. Current methods to handle distribution heterogeneity are to align clients’ distributions by adding additional modules such as Batch Normalization Li et al. [2021a], Mills et al. [2022], local model or local parameters Pillutla et al. [2022], regular term in loss function Hanzely et al. [2020], Li and Zhan [2021]. Or even re-train the model to remove the heterogeneous effects Zhang et al. [2023], Chen et al. [2023], Zhu et al. [2021]. All of them are trying to find the desired/important information that a client needs/provides and remove the noise/unwanted information. However, the lack of interpretability blocks the progress of PFL. Not only the efficiency but also the business model. People find it hard to measure clients’ contributions. This makes it difficult to allocate the benefits of PFL outcomes Zhou et al. [2021].

Interpretability of Deep Neural Network

There are two ways to categorize the interpretability methods. 1) The local explanation and the global explanation. Local explanation focuses on the behavior of a neural network towards an individual sample while global explanation gives an overview of a network’s knowledge Achtibat et al. [2023]. But local explanations can be aggregated to a global explanation Mor et al. [2024]. So we propose a local explanation method. 2) Feature-attribution-based and Concept-based explanation. Feature-attribution-based methods focus on “where” influences the network instead of “what”. The most popular feature attribution methods are to generate a saliency map that highlights the relevant features/pixels Sundararajan et al. [2017], Yang et al. [2023a], Smilkov et al. [2017], Shrikumar et al. [2017], Selvaraju et al. [2017], Srinivas and Fleuret [2019], Bhalla et al. [2023], Simonyan et al. [2014], Yang et al. [2023b], Erion et al. [2021]. It is far from enough for PFL. Concept-based methods can provide detailed information but they need a pre-defined concept set Kim et al. [2018] or extract the concept from the entire dataset Fel et al. [2023], Ghorbani et al. [2019]. Additionally, their costs are high Fel et al. [2023], Sun et al. [2023]. These shortcomings make current concept-based methods unsuitable for PFL due to the distributed privacy datasets and the uneven computational resources.

Method

We first model the neurons in the frequency domain and then propose our formula.

Neuron In Frequency Domain

Consider a classification dataset D with c classes as an example. We assume that the samples x_{ci} in dataset all has d features and denoted as $x_{ci} = (t_0, t_1, \dots, t_j)$. Additionally, we assume that every sample is generated by signal generator $f_c(\cdot)$. We introduce a basic assumption from generative models Kingma and Welling [2014], that for every class of samples, they follow a certain distribution. Therefore, We consider each sample as a wave in the time/space domain, consisting of typical samples (those with the highest confidence) plus some noise. Then x_{ci} is replaced with $f_c(t, i)$.

With this view, the neuron operations are matched to time-series signal processing. We transform the neuron outputs into the frequency domain:

$$p = \sigma \left(\sum_t x(t) y(t) + B \right) \quad (2)$$

$$= \sigma \left(\sum_t \left(\sum_k X(k) e^{j\frac{2\pi}{N}tk} \right) \left(\sum_k Y(k) e^{j\frac{2\pi}{N}tk} \right) + B \right) \quad (3)$$

$$= \sigma \left(\sum_k X(k) Y^*(k) + B \right) \quad (4)$$

where k means the k -th frequency. Notice that $X(k) Y^*(k)$ is the mutual energy of two signals. Since the Fourier transform of the real number field is conjugate symmetric, therefore

$$E_{xy}^k = E_{yx}^k \quad (5)$$

where E_{xy}^k denotes the mutual energy of the k -th frequency signal. Further, we can give the information-theoretic perspective condition for neuronal activation.

$$\sum_k E_{xy}^k + B > 0 \quad (6)$$

$$2 \sum_k E_{xy}^k + 2B > 0 \quad (7)$$

$$\sum_k E_x^k + \sum_k E_y^k + 2 \sum_k E_{xy}^k - 2B > \sum_k E_x^k + \sum_k E_y^k \quad (8)$$

We define the $E_{xy}^k < 0$ as noise since it decreases the reaction of the neuron and we denote them as E_{xy}^n . In contrast, we define the $E_{xy}^k > 0$ as a feature signal and we denote them as E_{xy}^f . We separate them into the two sides of the inequality sign.

$$\sum_f (E_x^f + E_y^f + 2E_{xy}^f) + \sum_n (E_x^n + E_y^n + 2E_{xy}^n) + 2B > \sum_f (E_x^f + E_y^f) + \sum_n (E_x^n + E_y^n) \quad (9)$$

$$\frac{\sum_f (E_x^f + E_y^f + 2E_{xy}^f) + \sum_n (E_x^n + E_y^n + 2E_{xy}^n) + 2B}{\sum_n (E_x^n + E_y^n + 2E_{xy}^n)} > \frac{\sum_f (E_x^f + E_y^f) + \sum_n (E_x^n + E_y^n)}{\sum_n (E_x^n + E_y^n + 2E_{xy}^n)} \quad (10)$$

$$SNR + 1 + \frac{2B}{E^n} > \frac{E_x + E_y}{E^n} \quad (11)$$

$$SNR > \frac{E_x + E_y - 2B}{E^n} - 1 \quad (12)$$

Where SNR denotes the signal-to-noise ratio which is an essential property used in signal processing and information theory.

Theorem 0.1 *In an unbiased neuron, or a neuron with a negative bias or the bias is regarded as a feature with value 1, if the neuron is activated, the SNR after the compounding of signals is larger than the original ones.*

Proof 0.2 *According to the definition of mutual energy,*

$$E_{xy}^n < 0 \quad (13)$$

$$E_{xy}^f > 0 \quad (14)$$

$$\sqrt{E_x E_y} > |E_{xy}| \quad (15)$$

And since energy is larger than 0.

$$E_x + E_y > 2\sqrt{E_x E_y} > 2|E_{xy}| \quad (16)$$

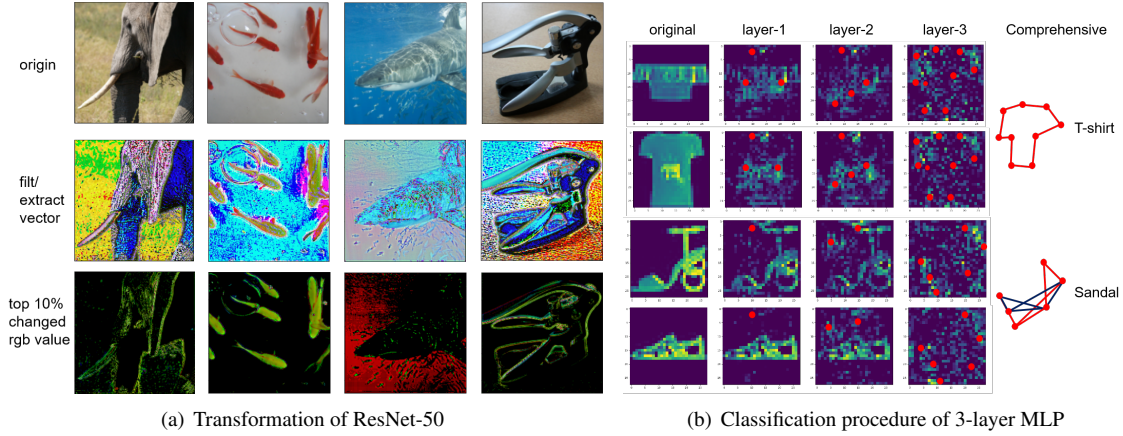


Figure 4: 4(a): The transformations of ResNet-50 towards a single sample of the imgNet dataset. 4(b): The classification procedure of a 3-layer MLP from the input layer to the output layer(left to right). The red points emphasize the similar transformations between the samples with the same label. Blue lines indicate that there are two kinds of sandals in FashionMNIST.

And let $B = 0$

$$SNR > \frac{E_x + E_y}{E_x^n + E_y^n + 2E_{xy}^n} - \frac{E_x^n + E_y^n + 2E_{xy}^n}{E_x^n + E_y^n + 2E_{xy}^n} \quad (17)$$

$$= \frac{E_x^f + E_y^f - 2E_{xy}^n}{E_x^n + E_y^n + 2E_{xy}^n} \quad (18)$$

Notice that $E_{xy}^n < 0$,

$$SNR > \frac{E_x^f + E_y^f - 2E_{xy}^n}{E_x^n + E_y^n + 2E_{xy}^n} > \frac{E_x^f + E_y^f}{E_x^n + E_y^n} = SNR_{origin} \quad (19)$$

Therefore, the forward procedure is a procedure that increases the SNR. If the network is well-trained.

SNR and Neuron

In classification tasks, the outputs from the same class become more and more similar as layers go deeperKonforti et al. [2023]. And the prior worksZhou et al. [2018], Sun et al. [2023] demonstrated that the samples with the same label have similar concepts. The neural network will act like an information selector that filters the unimportant informationKawaguchi et al. [2023]. If we regard each layer of neurons as a whole before the output goes through the amplitude limiter. The neurons are performing projective coordinate transformation. As prior work has observedKonforti et al. [2023], the samples with the same label have closer metrics in transformed space. So we define benchmark transformation according to the observation in Konforti et al. [2023]:

Definition 1: If the norm of vectors remain unchanged after transformation, we call this transformation benchmark transformation(It is also called Isometry).

With benchmark transformation, we define extract and filter operations which combine information bottleneck theory with spatial transformation:

Definition 2: If the norm of a vector is smaller/larger than the vector in benchmark transformation, we call this vector filtered/extracted. It is proven thatMoh [2020] M' with all vectors are unit vectors is a benchmark transformation. So, we compute filter/extract degree as the equations below:

$$\begin{aligned} deg &= \|v_{trans}\| - \|v_{origin}\| \\ &= (v_{ori}^T \cdot M)^T (v_{ori}^T \cdot M) - (v_{ori}^T \cdot M')^T (v_{ori}^T \cdot M') \end{aligned} \quad (20)$$

When $deg > 0$, it means this vector is extracted and otherwise filtered. Then we extend the definition to projection.

Definition 3: If the project of a vector v_1 on v_2 is smaller/larger than the corresponding project on $\frac{v_2}{\|v_2\|}$, we call this vector is filtered/extracted at the direct v_2 . We compute filter/extract degree as the equations below:

$$\begin{aligned} deg &= v_1^T \cdot v_2 - v_1^T \cdot \frac{v_2}{\|v_2\|} \\ &= v_1^T \cdot M_i - v_1^T \cdot M'_i \end{aligned} \quad (21)$$

Now we introduce the previous conclusion of activation functions into extract/filter definition. We can define the extract/filter operation of a neuron.

We first transform the weights of a neuron layer into benchmark transformation by dividing corresponding norms. The extract/filter operation of a neuron to a sample x can be written as (we regard bias as a feature with value 1):

$$deg = \sigma(x^T w) - x^T \frac{w}{\|w\|} \quad (22)$$

$$x' = x + \varepsilon \cdot deg \cdot w \quad (23)$$

This means the vector w of which neuron is responsible is extracted/filtered. We add the degree to the original sample to reveal how the network transforms the sample. The ε is the augmentation coefficient for downstream tasks such as generating more explicit figures in Fig.1. We adjust it according to the task requirements.

If there are n neurons in a layer, we calculate their mean:

$$x' = \left(\sum x'_i \right) / n \quad (24)$$

We regard each layer’s transformed x' as the outputs of the previous layer. So we can get the spatial transformation in the original space as shown in Fig.4 by performing the transformation from the output layer to the input layer. Fig.4(a) shows that similar concepts are transformed into nearby spaces such as “water(blue)”, “grass(green)” and “ground(yellow)”. As shown in line 3, the ResNet-50 has learned how to extract the shapes like specialized segment networks. Prior work Shotton et al. [2009], Li et al. [2021b] also demonstrated that shape is one of the most important decision factors. Fig.4(b) shows that no matter what shapes the original samples are, MLP will gradually transform them into a similar shape. *For pooling layer or other special layer, see Supplementary for details.*

| Method | Contain Texture | Batch Size | Time | Space (MB) | Need Entire Dataset | Need Auxiliary Model/Training |
|------------|-----------------|------------|----------------|------------|---------------------|-------------------------------|
| EAC | ✓ | 128 | >24h | 6660 | No | <u>Yes</u> |
| CRAFT | ✓ | 128 | >24h | 1566 | <u>Yes</u> | No |
| LPI | No | <u>32</u> | 13621.7s | ✗ | <u>Yes</u> | <u>Yes</u> |
| IntGrad | No | <u>4</u> | 6087.34s | ✗ | No | No |
| DeepLift | No | <u>64</u> | 522s | ✗ | No | No |
| FullGrad | No | <u>12</u> | 1857.36s | ✗ | No | No |
| InputGrad | No | 128 | 284.10s | 12294 | No | No |
| SmoothGrad | No | 128 | 6915.53s | 12212 | No | No |
| GradCam | No | 128 | 286.56s | 13122 | No | No |
| Ours | ✓ | 128 | 638.70s | 15862 | No | No |

Table 2: Functionality and Cost Comparison.

Experiments

In this section, we conduct 3 experiments to demonstrate that our proposal satisfies the limitations and conduct one experiment to demonstrate that our method can be adopted in FL and can be aggregated into a global explanation. The implementation details are contained in Supplementary.

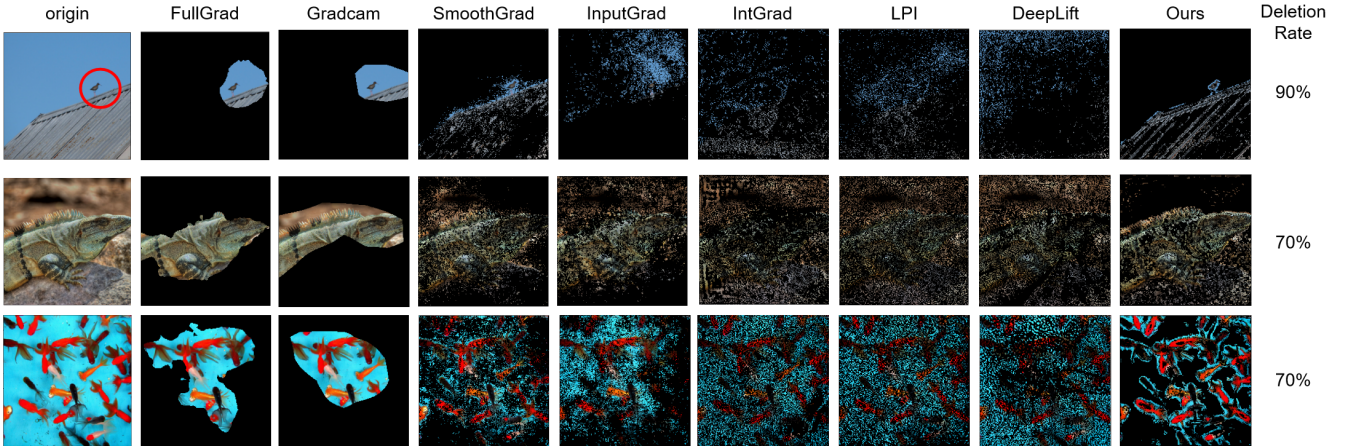


Figure 5: The results of the deletion and insertion game. The results of FullGrad and GradCAM are block-like because they smoothed their values. They perform well in most cases like the first example. However, when there are several important individuals such as the third example, they go wrong. But our method is more stable as displayed in this figure and the Figure.6.

Baselines: 1) Concept-based methods: EACSun et al. [2023], CRAFTFel et al. [2023], **2) Feature attribution-based methods: Integrated-based:** LPIYang et al. [2023a], IntGradSundararajan et al. [2017], **Perturbation-based:** SmoothGradSmilkov et al. [2017], **Back-propagation-based:** DeepLiftShrikumar et al. [2017], **Gradient \times input-based:** InputGradSimonyan et al. [2014], **Other:** GradCAMSelvaraju et al. [2017], FullGradSrinivas and Fleuret [2019]

Settings:In the first 3 experiments, we adopt the validation set of imgNetRussakovsky et al. [2015] and ResNet-50 as the backbone network. All of them are implemented on RTX 3090 24GB. See Supplementary for more details.

Functionality and Cost Comparison

In this part, we compared our method to current mainstream interpretability methods in terms of costs and functionalities to demonstrate that FreqX satisfies **the limitation1 and limitation3**. We set the batch size as 128 for all algorithms unless they exceed the capability of GPU.

As shown in Table.2. Current concept-based methods both have an extremely large time cost to explain the whole dataset. Additionally, they are based on the entire dataset to extract concept sets or auxiliary models/-training to separate concepts from the picture. Both of these two ways are costly and unsuitable for PFL. As for feature attribution methods, they can only find important areas. Some of them require even larger space than concept-based methods. And most of them need over 1000 seconds. Therefore, our method is more suitable for PFL because of its comprehensive functionalities and lower costs.(**limitation1** and **limitation3**)

Faithfulness Analysis

This experiment aims to demonstrate that our method can be transformed into a feature attribution method and to analyze the faithfulness of the method.

Metrics:The metrics of faithfulness are still ongoingYang et al. [2023a], Deng et al. [2024]. We adopt one of the earliest and most popular metrics which has been used until now. *Deletion and insertion game measure*Srinivas and Fleuret [2019]. This measure originates from game theory with the assumption that if we remove the most important part of the networks' decision-making basis, the output of the networks will change significantly. However, Srinivas and Fleuret [2019] argued that removing the most important pixels will create artifacts that puzzle networks. They suggested removing the least important pixels. To comprehensively evaluate the methods, we perform both versions: *delete least important pixel* and *delete most important pixel*. We evaluate the algorithms by removing the top/least $K\%$ important pixels. In the top $K\%$ part, **the lower** the curve is the better, while in the least $K\%$ part, **the higher** the better.

According to the spatial transformation, we find out that the important and unimportant pixels have different transformation properties. Based on this we design our algorithm to extract important pixels. To show the faith-

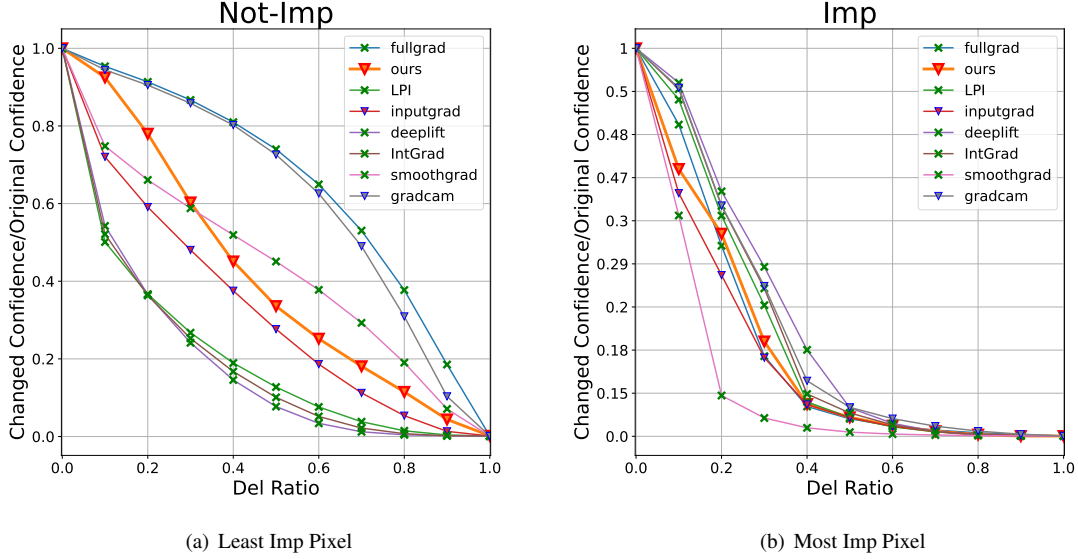


Figure 6: The Faithfulness Analysis. The line with green crosses means this method exceeds the capacity of the GPU or requires more than 1000 seconds. The orange line with large red triangles denotes our method. The line with blue triangles means their costs are affordable. The x-axis means the deletion rate of a picture and the y-axis means the corresponding changing rate of output.

fulness of FreqX, we set $\varepsilon = 1$ in this experiment to maintain the original transformation. See Supplementary for details.

Fig.5 shows the results of the deletion and insertion game. Fig.6 shows that our algorithm performs stably in both versions. Only Smooth-Grad and Full-Grad are better than us. **However**, Smooth-Grad takes 10 times running time than ours while Full-Grad **exceeds the capability of GPU** and takes 3 times running time than ours. Moreover, none of these feature attribution methods can explain the concept information. Therefore, **only our proposal can adapt to Personalized FL.(limitation1,2,3)**

Concept and Parameter Analysis

To the best of our knowledge, **NO CURRENT** concept-based method is affordable for PFL. Therefore, this experiment focuses on demonstrating the advantages compared to the attribution-based methods(**limitation2**). We design this experiment with the following assumption:

The current concept-based algorithms can extract concepts with a reasonable degree of accuracy. If our method can extract concepts too, we should have more similar results than those that cannot.

Based on this, we choose CRAFTFeI et al. [2023] as our benchmark concept-based method. CRAFT first separates the pictures into several pieces and regards them as pre-defined concepts. Then it clusters the concepts into groups and calculates their importance. For more details, turn to their paper. We separate the pictures in the same way. Details are displayed in the supplementary.

This experiment aims to demonstrate that spatial transformation contains concept information rather than strike for accuracy. We perform the K-means cluster algorithm directly in **original sample space**. We repeat the clustering 5 times and record their maximum and average values. After clustering the extracted concepts, we rank their importance by the algorithms we used in faithfulness analysis. Then we compare the results to CRAFT.

We set two methods g_1, g_2 for **ablation analysis** to demonstrate that spatial transformation does extract the concepts. g_1 does not perform the spatial transformation algorithm but it calculates the importance scores. And g_2 randomly selects the top concepts.

Metrics: All methods extract ten groups of concepts. We rank the groups according to their importance value. We select the top ten concepts of each group to compare their similarity. We design three measures. **1)** The number N of overlapping concepts of the corresponding group. **2)** The number M of overlapping concepts of all selected concepts. **3)** The hit rate N/M . We repeat the experiment 15 times and each time we randomly

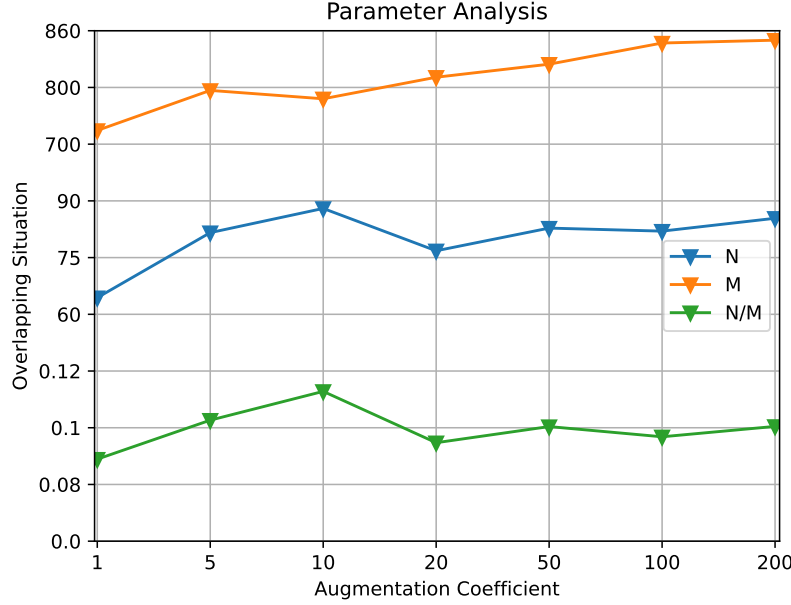


Figure 7: Parameter Analysis

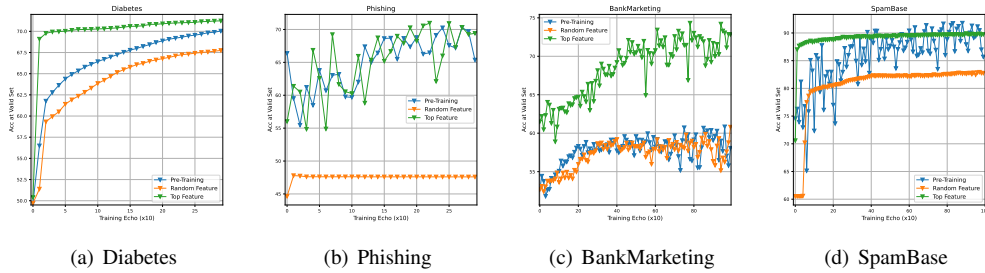


Figure 8: The testing accuracy of datasets. We repeat the experiment three times and calculate their mean value.

choose 50 classes from imgNet dataset. According to the results of faithfulness analysis, the transformed values of RGB range from -100 to 100 . We set $\varepsilon = 100$ in this experiment.

Analysis of ε : Theoretically, important information and noise information will be transformed at the same time. But important information will be transformed into nearby spaces while noise information will be transformed into anywhere in any layer. It means important information has a more intense transformation vector than noise information. Therefore, we set ε larger than the maximum value of the original transformation to resist the noise information. Fig.7 shows that our analysis is correct because when ε goes larger, the M , N , N/M all have an upward trend. And when $\varepsilon \geq 100$ the change becomes smaller.

Table.3 shows that our method has more overlapping concepts and a higher hit rate than the others. Our **average** values of M are close to their **maximum** values. The higher hit rate means that the increase of N is not the only reason for the increase of M . The spatial transformation is working. As for contrast groups, even though the importance is calculated the hit rate is **no better than the random selection**. This indicates that the feature attribution method can only find out the important area so that M increased. Without spatial transformation, they can not cluster similar concepts. The surpassing of our algorithm demonstrates that **our explanation result contains concept information**(*limitation2*).

Effectiveness

To demonstrate that our interpretability method can be aggregated into a **global explanation** and adopted into **federated learning**, we conduct a classic vertical federated learning scenario to calculate the contribution of

| Method | N | M | N/M |
|------------|--------------|---------------|---------------|
| Ours | 83.69 | 826.07 | 10.13% |
| g_1 | 64.22 | 693.49 | 9.26% |
| g_2 | 55.87 | 563.01 | 9.92% |
| InputGrad | 67.65 | 732.08 | 9.26% |
| GradCAM | 68.17 | 704.95 | 9.66% |
| FullGrad | 70.85 | 740.36 | 9.57% |
| DeepLift | 52.97 | 543.53 | 9.75% |
| SmoothGrad | 70.25 | 771.43 | 9.11% |
| IntGrad | 53.67 | 559.01 | 9.59% |
| LPI | 57.40 | 579.21 | 9.92% |
| Max | N | M | N/M |
| Ours | 162 | 926.07 | 17.49% |
| g_1 | 133.73 | 800.87 | 16.70% |
| g_2 | 117.33 | 742.33 | 15.81% |
| InputGrad | 133 | 845.6 | 15.74% |
| GradCAM | 133.6 | 823.27 | 16.22% |
| FullGrad | 139.93 | 856.67 | 16.34% |
| DeepLift | 107.67 | 649.6 | 16.57% |
| SmoothGrad | 139.93 | 889.73 | 15.72% |
| IntGrad | 109.47 | 668.4 | 16.37% |
| LPI | 115.13 | 686.67 | 16.78% |

Table 3: The average and maximum value of experiments.

participants. We implement a classic Shapley value-based algorithm which is widely used in federated learning as baseline Zhou et al. [2021]. It is necessary to mention that this experiment aims to show the **potential ability** of our algorithm rather than proving the efficiency.

This experiment has two steps. In the first step, we aggregate our explanation result into a global explanation and test the feature evaluation ability of our method. In the second step, we use the feature evaluation ability to calculate the contribution of each client and compare the result to the classic Shapley value-based algorithm. According to the properties of the datasets, we set $\varepsilon = 1000$ to resist the noises.

In this experiment, we adopt four popular tabular datasets.

- **DiabetesNR** et al. [2017], a popularly used dataset made by CDC with 253680 instances and 21 features. It is also used in prior work.Wang et al. [2022]
- **PhishingRami** and Lee [2015], Dataset that provides relevant features for determining if a website is a phishing website. Contains 11,055 samples each with 111 features. It is also used in prior workCastiglia et al. [2023].
- **BankMarketingS**. et al. [2012], Dataset that provides relevant features for determining if a client is willing to participate in Portuguese Bank’s products. Contains 41188 instances and 16 features.
- **SpamBaseMark** et al. [1999].Dataset that provides relevant features for determining whether an email is spam or not. Contains 4601 instances and 57 features.

Note that not all the features in the original dataset are necessarily significant. We adopt a 3-layer MLP as a backbone network to classify the datasets.

Step 1: We first pre-train the MLP with all features and select the top-10 features to re-train the MLP. For comparison, we randomly select 10 features and re-train the model. We use the following equations to calculate the importance score of a feature in which c denotes the number of classes, n_c denotes the sample amount in class c , j denotes the j -th feature, \mathbf{x}' denotes the sample point after spatial transformation while \mathbf{x} denotes the

| Dataset | Number of Overlapping Ranks | Baseline |
|---------------|-----------------------------|----------|
| Phishing | 1.2 | 1 |
| BankMarketing | 1.35 | 1 |
| SpamBase | 1.25 | 1 |
| Diabetes | 1.25 | 1 |
| Average | 1.2625 | 1 |

Table 4: The number overlapping ranks between our method and Shapley value-based method. The baseline values are calculated by the probability theory if there is no relevance between the two methods.

original sample point.

$$\vec{v}_c = \left(\sum_i^{n_c} \mathbf{x}'_i - \mathbf{x}_i \right) \div n_c \quad (25)$$

$$s_j = abs \left(\prod_{i=0}^c \vec{v}_{cj} \right) \quad (26)$$

Fig.8 shows that the model with our selection algorithm converges faster and even more accurately in some cases. In contrast, with random selection, the model converges slower and the accuracy decreases. This demonstrates that our algorithm **can be aggregated into a global explanation and distinguish the important features**.

Step 2: For each dataset, we evenly and randomly allocate the features to 3 clients. We first perform the baseline to get the contribution rank of clients. Then we calculate the clients’ contribution with our importance score and rank the clients too. The details of the experiment are introduced in Supplementary. After repeating the experiment 20 times we have the results shown in Table.4.

Table.4 shows that our method has more overlapping ranks than the baseline which indicates that our method has relevance with Shapley value. This result shows that our method has the potential to be applied in federated learning. *It is worth emphasizing our method only needs to pre-train once, while the Shapley value-based method has to train multiple times due to the different partition ways of clients.*

Conclusion

We present a novel interpretability method for personalized federated learning, addressing the challenge of imbalanced computational resources. Our experiments validate the method’s cost-effectiveness and performance. A significant contribution is the identification of neural network spatial transformations that capture both attribute and conceptual information, demonstrated through two independent experiments. We further establish the method’s relevance in federated learning by drawing a connection to the Shapley value approach and emphasizing its lower cost profile. We contribute to the field by offering a practical, economically viable solution that enhances interpretability without compromising performance.

References

Reduan Achtibat, Maximilian Dreyer, Ilona Eisenbraun, Sebastian Bosse, Thomas Wiegand, Wojciech Samek, and Sebastian Lapuschkin. From attribution maps to human-understandable explanations through concept relevance propagation. *Nat. Mac. Intell.*, 5(9), 2023. doi: 10.1038/S42256-023-00711-8.

Alexander A. Alemi, Ian Fischer, Joshua V. Dillon, and Kevin Murphy. Deep variational information bottleneck. In *5th International Conference on Learning Representations, ICLR 2017*, 2017. URL <https://openreview.net/forum?id=HyxQzBceg>.

Usha Bhalla, Suraj Srinivas, and Himabindu Lakkaraju. Discriminative feature attributions: Bridging post hoc explainability and inherent interpretability. In Alice Oh, Tristan Naumann, Amir Globerson, Kate Saenko, Moritz Hardt, and Sergey Levine, editors, *Advances in Neural Information Processing Systems 36: Annual Conference on Neural Information Processing Systems 2023, NeurIPS 2023*, 2023.

- Timothy Castiglia, Yi Zhou, Shiqiang Wang, Swanand Kadhe, Nathalie Baracaldo, and Stacy Patterson. LESS-VFL: communication-efficient feature selection for vertical federated learning. In Andreas Krause, Emma Brunskill, Kyunghyun Cho, Barbara Engelhardt, Sivan Sabato, and Jonathan Scarlett, editors, *International Conference on Machine Learning, ICML 2023*, volume 202 of *Proceedings of Machine Learning Research*, 2023.
- Bhaskar Ray Chaudhury, Linyi Li, Mintong Kang, Bo Li, and Ruta Mehta. Fairness in federated learning via core-stability. In Sanmi Koyejo, S. Mohamed, A. Agarwal, Danielle Belgrave, K. Cho, and A. Oh, editors, *Advances in Neural Information Processing Systems 35: Annual Conference on Neural Information Processing Systems 2022, NeurIPS 2022*, 2022. URL http://papers.nips.cc/paper_files/paper/2022/hash/25e92e33ac8c35fd49f394c37f21b6da-Abstract-Conference.html.
- Huancheng Chen, Chianing Wang, and Haris Vikalo. The best of both worlds: Accurate global and personalized models through federated learning with data-free hyper-knowledge distillation. In *The Eleventh International Conference on Learning Representations, ICLR 2023*, 2023. URL <https://openreview.net/pdf?id=29V3AWjVAFi>.
- Huiqi Deng, Na Zou, Mengnan Du, Weifu Chen, Guocan Feng, Ziwei Yang, Zheyang Li, and Quanshi Zhang. Unifying fourteen post-hoc attribution methods with taylor interactions. *IEEE Transactions on Pattern Analysis and Machine Intelligence*, 46(7), 2024. doi: 10.1109/TPAMI.2024.3358410.
- Gabriel G. Erion, Joseph D. Janizek, Pascal Sturmfels, Scott M. Lundberg, and Su-In Lee. Improving performance of deep learning models with axiomatic attribution priors and expected gradients. *Nat. Mach. Intell.*, 3(7), 2021. doi: 10.1038/S42256-021-00343-W.
- Thomas Fel, Agustin Martin Picard, Louis Béthune, Thibaut Boissin, David Vigouroux, Julien Colin, Rémi Cadène, and Thomas Serre. CRAFT: concept recursive activation factorization for explainability. In *IEEE/CVF Conference on Computer Vision and Pattern Recognition, CVPR 2023*, 2023. doi: 10.1109/CVPR52729.2023.00266.
- Liang Gao, Huazhu Fu, Li Li, Yingwen Chen, Ming Xu, and Cheng-Zhong Xu. Feddc: Federated learning with non-iid data via local drift decoupling and correction. In *IEEE/CVF Conference on Computer Vision and Pattern Recognition, CVPR 2022*, 2022. doi: 10.1109/CVPR52688.2022.00987.
- Amirata Ghorbani, James Wexler, James Y. Zou, and Been Kim. Towards automatic concept-based explanations. In Hanna M. Wallach, Hugo Larochelle, Alina Beygelzimer, Florence d’Alché-Buc, Emily B. Fox, and Roman Garnett, editors, *Advances in Neural Information Processing Systems 32: Annual Conference on Neural Information Processing Systems 2019, NeurIPS 2019*, 2019.
- Filip Hanzely, Slavomír Hanzely, Samuel Horváth, and Peter Richtárik. Lower bounds and optimal algorithms for personalized federated learning. In Hugo Larochelle, Marc’Aurelio Ranzato, Raia Hadsell, Maria-Florina Balcan, and Hsuan-Tien Lin, editors, *Advances in Neural Information Processing Systems 33: Annual Conference on Neural Information Processing Systems 2020, NeurIPS 2020*, 2020. URL <https://proceedings.neurips.cc/paper/2020/hash/187acf7982f3c169b3075132380986e4-Abstract.html>.
- Jun Deng Jianxun Zhao. *Fundamentals of Radio Frequency Circuits*. Xidian University Press, 2018.
- Kenji Kawaguchi, Zhun Deng, Xu Ji, and Jiaoyang Huang. How does information bottleneck help deep learning? In Andreas Krause, Emma Brunskill, Kyunghyun Cho, Barbara Engelhardt, Sivan Sabato, and Jonathan Scarlett, editors, *International Conference on Machine Learning, ICML 2023*, volume 202 of *Proceedings of Machine Learning Research*, 2023. URL <https://proceedings.mlr.press/v202/kawaguchi23a.html>.
- Been Kim, Martin Wattenberg, Justin Gilmer, Carrie J. Cai, James Wexler, Fernanda B. Viégas, and Rory Sayres. Interpretability beyond feature attribution: Quantitative testing with concept activation vectors (TCAV). In Jennifer G. Dy and Andreas Krause, editors, *Proceedings of the 35th International Conference on Machine Learning, ICML 2018*, volume 80 of *Proceedings of Machine Learning Research*, 2018.
- Diederik P. Kingma and Max Welling. Auto-encoding variational bayes. In Yoshua Bengio and Yann LeCun, editors, *2nd International Conference on Learning Representations, ICLR 2014*, 2014. URL <http://arxiv.org/abs/1312.6114>.

- Yael Konforti, Alon Shpigler, Boaz Lerner, and Aharon Bar-Hillel. SIGN: statistical inference graphs based on probabilistic network activity interpretation. *IEEE Trans. Pattern Anal. Mach. Intell.*, 45(3), 2023. doi: 10.1109/TPAMI.2022.3181472.
- Dan Ley, Saumitra Mishra, and Daniele Magazzeni. GLOBE-CE: A translation based approach for global counterfactual explanations. In Andreas Krause, Emma Brunskill, Kyunghyun Cho, Barbara Engelhardt, Sivan Sabato, and Jonathan Scarlett, editors, *International Conference on Machine Learning, ICML 2023*, volume 202 of *Proceedings of Machine Learning Research*, 2023. URL <https://proceedings.mlr.press/v202/ley23a.html>.
- Peichun Li, Guoliang Cheng, Xumin Huang, Jiawen Kang, Rong Yu, Yuan Wu, and Miao Pan. Anycostfl: Efficient on-demand federated learning over heterogeneous edge devices. In *IEEE INFOCOM 2023 - IEEE Conference on Computer Communications*, 2023. doi: 10.1109/INFOCOM53939.2023.10229017.
- Tian Li, Anit Kumar Sahu, Manzil Zaheer, Maziar Sanjabi, Ameet Talwalkar, and Virginia Smith. Federated optimization in heterogeneous networks. In Inderjit S. Dhillon, Dimitris S. Papailiopoulos, and Vivienne Sze, editors, *Proceedings of the Third Conference on Machine Learning and Systems, MLSys 2020, Austin, TX, USA, March 2-4, 2020*, 2020. URL https://proceedings.mlsys.org/paper_files/paper/2020/hash/1f5fe83998a09396ebe6477d9475ba0c-Abstract.html.
- Xiaoxiao Li, Meirui Jiang, Xiaofei Zhang, Michael Kamp, and Qi Dou. Fedbn: Federated learning on non-iid features via local batch normalization. In *9th International Conference on Learning Representations, ICLR 2021*, 2021a. URL <https://openreview.net/forum?id=6YEQUn0QICG>.
- Xin-Chun Li and De-Chuan Zhan. Fedrs: Federated learning with restricted softmax for label distribution non-iid data. In Feida Zhu, Beng Chin Ooi, and Chunyan Miao, editors, *KDD '21: The 27th ACM SIGKDD Conference on Knowledge Discovery and Data Mining, Virtual Event, 2021*, 2021. doi: 10.1145/3447548.3467254.
- Yingwei Li, Qihang Yu, Mingxing Tan, Jieru Mei, Peng Tang, Wei Shen, Alan L. Yuille, and Cihang Xie. Shapetexture debiased neural network training. In *9th International Conference on Learning Representations, ICLR 2021*, 2021b. URL <https://openreview.net/forum?id=Db4yerZTYkz>.
- "Hopkins Mark, Reeber Erik, Forman George, and Suermondt Jaap". Spambase. UCI Machine Learning Repository, 1999. DOI: <https://doi.org/10.24432/C53G6X>.
- Brendan McMahan, Eider Moore, Daniel Ramage, Seth Hampson, and Blaise Agüera y Arcas. Communication-efficient learning of deep networks from decentralized data. In Aarti Singh and Xiaojin (Jerry) Zhu, editors, *Proceedings of the 20th International Conference on Artificial Intelligence and Statistics, AISTATS 2017*, volume 54 of *Proceedings of Machine Learning Research*, 2017. URL <http://proceedings.mlr.press/v54/mcmahan17a.html>.
- Jed Mills, Jia Hu, and Geyong Min. Multi-task federated learning for personalised deep neural networks in edge computing. *IEEE Trans. Parallel Distributed Syst.*, 33(3), 2022. doi: 10.1109/TPDS.2021.3098467.
- Tzuong-Tsieng Moh. *Linear Algebra and Its Applications*, volume 10 of *Series on University Mathematics*. WorldScientific, 2020. ISBN 9789813235427. doi: 10.1142/10861.
- Alon Mor, Yonatan Belinkov, and Benny Kimelfeld. Accelerating the global aggregation of local explanations. In Michael J. Wooldridge, Jennifer G. Dy, and Sriraam Natarajan, editors, *Thirty-Eighth AAAI Conference on Artificial Intelligence, AAAI 2024*, 2024. doi: 10.1609/AAAI.V38I17.29845.
- Burrows NR, Hora I, Geiss LS, Gregg EW, and Albright A. "incidence of end-stage renal disease attributed to diabetes among persons with diagnosed diabetes — united states and puerto rico". *MMWR Morb Mortal Wkly Rep*, 2017. doi: "10.15585/mmwr.mm6643a2". URL "http://dx.doi.org/10.15585/mmwr.mm6643a2".
- Krishna Pillutla, Kshitiz Malik, Abdelrahman Mohamed, Michael Rabbat, Maziar Sanjabi, and Lin Xiao. Federated learning with partial model personalization. In Kamalika Chaudhuri, Stefanie Jegelka, Le Song, Csaba Szepesvári, Gang Niu, and Sivan Sabato, editors, *International Conference on Machine Learning, ICML 2022*, volume 162 of *Proceedings of Machine Learning Research*, 2022. URL <https://proceedings.mlr.press/v162/pillutla22a.html>.

- Yulei Qin, Xingyu Chen, Chao Chen, Yunhang Shen, Bo Ren, Yun Gu, Jie Yang, and Chunhua Shen. Fopro: Few-shot guided robust webly-supervised prototypical learning. In Brian Williams, Yiling Chen, and Jennifer Neville, editors, *Thirty-Seventh AAAI Conference on Artificial Intelligence, AAAI 2023*, 2023a. doi: 10.1609/AAAI.V37I2.25303.
- Yulei Qin, Xingyu Chen, Yunhang Shen, Chaoyou Fu, Yun Gu, Ke Li, Xing Sun, and Rongrong Ji. Capro: Webly supervised learning with cross-modality aligned prototypes. In Alice Oh, Tristan Naumann, Amir Globerson, Kate Saenko, Moritz Hardt, and Sergey Levine, editors, *Advances in Neural Information Processing Systems 36: Annual Conference on Neural Information Processing Systems 2023, NeurIPS 2023*, 2023b. URL http://papers.nips.cc/paper_files/paper/2023/hash/a7e0d77325db843fd5baf1298163e89a-Abstract-Conference.html.
- Taki Hasan Rafi, Faiza Anan Noor, Tahmid Hussain, and Dong-Kyu Chae. Fairness and privacy preserving in federated learning: A survey. *Inf. Fusion*, 105, 2024. doi: 10.1016/J.INFFUS.2023.102198.
- Mohammad Rami and McCluskey Lee. Phishing Websites. UCI Machine Learning Repository, 2015. DOI: <https://doi.org/10.24432/C51W2X>.
- Olga Russakovsky, Jia Deng, Hao Su, Jonathan Krause, Sanjeev Satheesh, Sean Ma, Zhiheng Huang, Andrej Karpathy, Aditya Khosla, Michael S. Bernstein, Alexander C. Berg, and Li Fei-Fei. Imagenet large scale visual recognition challenge. *Int. J. Comput. Vis.*, 115(3), 2015. doi: 10.1007/S11263-015-0816-Y. URL <https://doi.org/10.1007/s11263-015-0816-y>.
- Moro S., Rita P., and Cortez P. Bank Marketing. UCI Machine Learning Repository, 2012. DOI: <https://doi.org/10.24432/C5K306>.
- Ramprasaath R. Selvaraju, Michael Cogswell, Abhishek Das, Ramakrishna Vedantam, Devi Parikh, and Dhruv Batra. Grad-cam: Visual explanations from deep networks via gradient-based localization. In *IEEE International Conference on Computer Vision, ICCV 2017*, 2017. doi: 10.1109/ICCV.2017.74.
- Jamie Shotton, John M. Winn, Carsten Rother, and Antonio Criminisi. Textonboost for image understanding: Multi-class object recognition and segmentation by jointly modeling texture, layout, and context. *Int. J. Comput. Vis.*, 81(1), 2009. doi: 10.1007/S11263-007-0109-1.
- Avanti Shrikumar, Peyton Greenside, and Anshul Kundaje. Learning important features through propagating activation differences. In Doina Precup and Yee Whye Teh, editors, *Proceedings of the 34th International Conference on Machine Learning, ICML 2017*, volume 70 of *Proceedings of Machine Learning Research*, 2017.
- Karen Simonyan, Andrea Vedaldi, and Andrew Zisserman. Deep inside convolutional networks: Visualising image classification models and saliency maps. In Yoshua Bengio and Yann LeCun, editors, *2nd International Conference on Learning Representations, ICLR 2014*, 2014.
- Daniel Smilkov, Nikhil Thorat, Been Kim, Fernanda B. Viégas, and Martin Wattenberg. Smoothgrad: removing noise by adding noise. *CoRR*, abs/1706.03825, 2017. URL <http://arxiv.org/abs/1706.03825>.
- Steven W. Smith. *The Scientist and Engineer Guide to Digital Signal Processing*. California Technical Publishing, 1997.
- Suraj Srinivas and François Fleuret. Full-gradient representation for neural network visualization. In Hanna M. Wallach, Hugo Larochelle, Alina Beygelzimer, Florence d’Alché-Buc, Emily B. Fox, and Roman Garnett, editors, *Advances in Neural Information Processing Systems 32: Annual Conference on Neural Information Processing Systems 2019, NeurIPS 2019*, 2019.
- Ao Sun, Pingchuan Ma, Yuanyuan Yuan, and Shuai Wang. Explain any concept: Segment anything meets concept-based explanation. In Alice Oh, Tristan Naumann, Amir Globerson, Kate Saenko, Moritz Hardt, and Sergey Levine, editors, *Advances in Neural Information Processing Systems 36: Annual Conference on Neural Information Processing Systems 2023, NeurIPS 2023*, 2023.
- Mukund Sundararajan, Ankur Taly, and Qiqi Yan. Axiomatic attribution for deep networks. In Doina Precup and Yee Whye Teh, editors, *Proceedings of the 34th International Conference on Machine Learning, ICML 2017*, volume 70 of *Proceedings of Machine Learning Research*, 2017.

- Junhao Wang, Lan Zhang, Anran Li, Xuanke You, and Haoran Cheng. Efficient participant contribution evaluation for horizontal and vertical federated learning. In *38th IEEE International Conference on Data Engineering, ICDE 2022*, 2022. doi: 10.1109/ICDE53745.2022.00073.
- Logan G. Wright, Tatsuhiro Onodera, Martin M. Stein, Tianyu Wang, Darren T. Schachter, Zoey Hu, and Peter L. McMahon. Deep physical neural networks trained with backpropagation. *Nat.*, 601(7894), 2022. doi: 10.1038/S41586-021-04223-6.
- Chenhao Xu, Youyang Qu, Yong Xiang, and Longxiang Gao. Asynchronous federated learning on heterogeneous devices: A survey. *Comput. Sci. Rev.*, 50, 2023. doi: 10.1016/J.COSREV.2023.100595.
- Peiyu Yang, Naveed Akhtar, Zeyi Wen, and Ajmal Mian. Local path integration for attribution. In Brian Williams, Yiling Chen, and Jennifer Neville, editors, *Thirty-Seventh AAAI Conference on Artificial Intelligence, AAAI 2023, Thirty-Fifth Conference on Innovative Applications of Artificial Intelligence*, 2023a. doi: 10.1609/AAAI.V37I3.25422.
- Peiyu Yang, Naveed Akhtar, Zeyi Wen, Mubarak Shah, and Ajmal Saeed Mian. Re-calibrating feature attributions for model interpretation. In *The Eleventh International Conference on Learning Representations, ICLR 2023*, 2023b.
- Jianqing Zhang, Yang Hua, Hao Wang, Tao Song, Zhengui Xue, Ruhui Ma, and Haibing Guan. Fedala: Adaptive local aggregation for personalized federated learning. In Brian Williams, Yiling Chen, and Jennifer Neville, editors, *Thirty-Seventh AAAI Conference on Artificial Intelligence, AAAI 2023*, 2023. doi: 10.1609/AAAI.V37I9.26330.
- Bolei Zhou, Yiyou Sun, David Bau, and Antonio Torralba. Interpretable basis decomposition for visual explanation. In Vittorio Ferrari, Martial Hebert, Cristian Sminchisescu, and Yair Weiss, editors, *Computer Vision - ECCV 2018 - 15th European Conference*, volume 11212 of *Lecture Notes in Computer Science*, 2018. doi: 10.1007/978-3-030-01237-3_8.
- Zirui Zhou, Lingyang Chu, Changxin Liu, Lanjun Wang, Jian Pei, and Yong Zhang. Towards fair federated learning. In Feida Zhu, Beng Chin Ooi, and Chunyan Miao, editors, *KDD '21: The 27th ACM SIGKDD Conference on Knowledge Discovery and Data Mining, Virtual Event, 2021*, 2021. doi: 10.1145/3447548.3470814.
- Zhuangdi Zhu, Junyuan Hong, and Jiayu Zhou. Data-free knowledge distillation for heterogeneous federated learning. In Marina Meila and Tong Zhang, editors, *Proceedings of the 38th International Conference on Machine Learning, ICML 2021*, volume 139 of *Proceedings of Machine Learning Research*, 2021. URL <http://proceedings.mlr.press/v139/zhu21b.html>.